RESEARCH AND DEVELOPMENT BRANCH
DEPARTMENT OF NATIONAL DEFENCE
CANADA

DEFENCE RESEARCH ESTABLISHMENT OTTAWA

DREO REPORT NO. 818
DREO ~~R~~ 818

MEASUREMENTS AND CALCULATIONS OF THE THERMAL RESISTANCE OF THREE SYNTHETIC-FIBRE BATTINGS

by

B. Farnworth, R.M. Crow and M.M. Dewar

NOVEMBER 1979
OTTAWA

(3)

RESEARCH AND DEVELOPMENT BRANCH

DEPARTMENT OF NATIONAL DEFENCE
CANADA

DEFENCE RESEARCH ESTABLISHMENT OTTAWA

DREO REPORT NO. 818

(6)

MEASUREMENTS AND CALCULATIONS OF THE THERMAL RESISTANCE OF THREE SYNTHETIC-FIBRE BATTINGS

by

(10) B. Farnworth, R.M. Crow and M.M. Dewar
Environmental Protection Section
Protective Sciences Division

(14) DREO-818

(12) 36

(11) NOVEMBER 1979
OTTAWA

404576 LB

ABSTRACT

A theory of the combined transport of heat by radiation and by conduction in fibrous media is presented. The theory agrees well with the measured thermal resistance of three insulating battings and explains the differences between them without the inclusion of convective heat transfer being required.

RÉSUMÉ

On présente ici une théorie qui explique deux moyens de transport du chaleur à travers les tissus fibreux. Cette théorie fournit une explication des différences entre les resultats obtenus pour les resistances thermiques de trois tissus isolants, sans besoin de se servir d'un facteur de correction pour la convection.

TABLE OF CONTENTS

INTRODUCTION

Heat can propagate across a dry textile insulant or batting in four ways: conduction along the fibres, conduction by the entrapped air, radiation and convection in the air. It is generally found that the transmission of heat across such insulants is greater than can be accounted for by conduction along the fibres and through the air alone. The excess is usually attributed to convection.

Recently a new insulating material, Thinsulate, has been introduced by the 3M Company Ltd. It is composed of extremely fine polyolefin fibres and has a thermal resistance about one-and-a-half times that of conventional battings. We have theorized that this greater thermal resistance is due to reduced heat transfer by radiation. In order to confirm this hypothesis, the following study was undertaken.

First, a theoretical model was developed to include heat transfer by conduction and radiation. The essential features of the model are that the absorption and emission of thermal radiation by individual fibres are considered explicitly and that the radiative and conductive heat transfer mechanisms are treated simultaneously by a coupled set of differential equations. Second, experiments were carried out to determine values for the unknown parameters presented in the model. Once these values were established, the theoretical and experimental values of thermal resistance were compared for two types of conventional battings and for Thinsulate at varying thicknesses and varying weights. The results indicate that conduction and radiation alone are sufficient to account for the observed heat transfer in all three battings and that the high resistance of Thinsulate is due to its higher opacity.

THEORY

The theory developed here makes simplifying assumptions, some of which cannot be justified in any fundamental sense but are justified in that they limit the parameters of the theory to easily measured physical quantities. For example, it is assumed that the fibres are themselves straight and that they lie randomly within the batting since to assume otherwise would not only greatly complicate the mathematics but would require precise knowledge of the actual fibre distribution. Similarly it is assumed that the density of the batting is uniform throughout. It is also assumed that the temperature within the batting varies only along the direction of net heat flow, i.e. perpendicular to the surfaces of the batting.

An implicit assumption is that heat flow by convection is negligible. This can only be justified by a comparison of the theoretical and experimental results for each batting.

CONDUCTIVE HEAT TRANSFER

Heat may be conducted across a layer of batting by either the fibres or the intervening air. A general calculation of the heat flow through such an air-fibre mixture would be exceedingly complex. In going from one side of the batting to the other, a flow line (i.e. a line that is everywhere parallel to the local heat flow) would spend some of its length in air, some inside fibres and would be anything but straight. However, the assumptions made here is that the temperature varies only in a direction perpendicular to the two batting surfaces. With this assumption, the calculation of the combined heat flow through the two media is simple and exact.

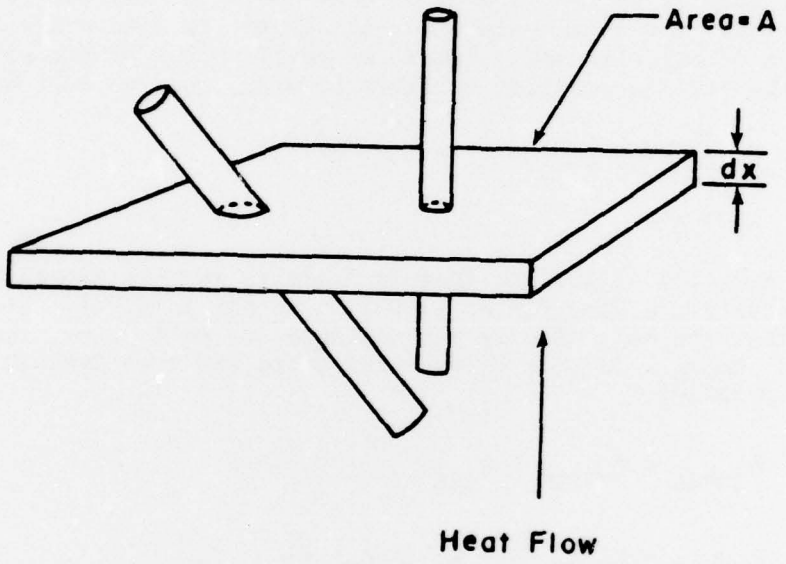

Figure 1. A thin slice through the batting intersects the fibres to give small cylinders of circular or elliptical cross-section.

Consider a thin slice of thickness dx and area A, cut through the batting parallel to its surfaces. This slice will intersect fibres at various angles, as illustrated in Figure 1. Assuming a uniform distribution of fibres, the fraction of the volume of this slice that is occupied by fibre is the same as for the batting as a whole, f, where $f \times 100$ is the percent fibre volume.

When viewed from the top or the bottom, the slice shows a circle or an ellipse where each fibre is intersected. The intersected volume of each fibre is the area of this circle or ellipse times the thickness dx. The total volume for all fibres is $A_F dx$ where A_F is the total area of all ellipses. Since the total volume of the slice is Adx and the portion occupied by fibre is Afdx, then we must have

$$A_F \, dx = Af \, dx$$

or $$A_F = Af$$

Thus the fraction of surface that is fibre is the fractional fibre volume f. Conversely the fraction of area that is air is (1-f). Since it is assumed that the heat flow is perpendicular to this slice, the total heat flow, Q_{TOTAL}, is that through the fibre and that through the air, added in parallel.

$$Q_{TOTAL} = Q_{FIBRE} + Q_{AIR}$$

$$= k_F \, A_F \frac{dT}{dx} + k_A \, (A-A_F) \frac{dT}{dx}$$

$$= k_F \, Af \frac{dT}{dx} + k_A \, (1-f) \, A \frac{dT}{dx}$$

(1) $$Q_{TOTAL} = A \frac{dT}{dx} \{ f k_F + (1-f) \, k_A \}$$

where k_F is the thermal conductivity of the fibre

k_A is the thermal conductivity of the air

and $\frac{dT}{dx}$ is the temperature gradient

Hence the combined thermal conductivity is

(2) $$k = f \, k_F + (1-f) \, k_A .$$

This result is the same as the one that would be obtained for a batting in which all the fibres are aligned parallel to the heat flow. This then gives a maximum value of combined conductivity and is probably unrealistic for large values of f. However the result is a direct consequence of the assumption of a unidirectional temperature gradient and is therefore necessary to the theory.

RADIATIVE HEAT FLOW

An experimental arrangement for the measurement of thermal resistances of battings is illustrated in Figure 2. The batting is held between two plates which are black, or nearly so, to thermal radiation. The two plates are at known temperatures not far removed from room temperature or 300 K, the difference in temperature between the two plates being of the order of 1 to 10 K. To a first approximation, the space between the plates occupied by the batting can be regarded as a cavity at about 300 K and will thus be filled by thermal radiation with a characteristic temperature of 300 K.

If one considers the radiant energy flowing through a plane intermediate to the two plates, this will be of the order of $\sigma < T>^4$ per unit time per unit area in each direction. Here σ is the Stefan-Boltzmann constant and $<T>$ is the average temperature of the apparatus. The total flux will then be about $2\sigma < T>^4$.

Now the net radiant heat flux will be the difference between the flows to the left and to the right and will depend on the temperature difference between the two plates. For a perfectly transparent medium this net flow is

$$\sigma \{< T> + \frac{\Delta T}{2}\}^4 - \sigma \{< T> - \frac{\Delta T}{2}\}^4$$

$$= \sigma < T>^4 \left[\frac{4\Delta T}{< T>} + \{\frac{\Delta T}{< T>}\}^3\right]$$

where ΔT is the temperature difference.

Since $\frac{\Delta T}{<T>} \cong \frac{10}{300} = \frac{1}{30}$

the term in $\left(\frac{\Delta T}{<T>}\right)^3$ can be neglected and the net heat flow is approximately $4\sigma <T>^3 \Delta T$. Comparing this to the total radiant heat flow

$$\frac{4\sigma <T>^3 \Delta T}{2\sigma <T>^4} = 2\frac{\Delta T}{<T>} \cong \frac{1}{15}$$

Thus the net heat flow is small (maximum value of 1/15 or 7%) compared to the total radiant heat flux. This condition is essential to the analysis that follows since it permits the assumption of a basically isotropic radiation field with only a small anisotropic component.

Consider a volume element dV within the fabric of area A and thickness dx as in Figure 3. This volume element will be irradiated from all directions with approximately the same intensity from any direction (Intensity is energy flow per unit time per unit area per unit solid angle) but with a slightly higher intensity from the hot side than from the other. Consider, for the moment, only the radiation from left to right. Let the total incident flux per unit area be $F_R(x)$. If the intensity is $I(x)$ then we can find $F_R(x)$ from $I(x)$ by integrating over all solid angles in the left-half space.

$$A\, F_R(x) = \int_0^{2\pi} d\phi \int_0^{\pi/2} d\theta \, \sin\theta \, I(x)\, A \cos\theta = \pi A\, I(x)$$

or

(3) $$F_R(x) = \pi\, I(x)$$

Of this incident radiation, a fraction will be absorbed by the fibres in dV. Suppose the fibres are of length L and radius R, and there are n per unit volume. Then L, R and n can be related to the fractional fibre volume by

(4) $$n\pi R^2 L = f$$

Radiation incident on dV from any angle will encounter a volume of fibre fAdx. If we assume that the fibre density is low so that the fibres do not significantly shadow one another, then from any angle the radiation will see the same amount of absorbing surface. If a fibre happens to be lined up perpendicular to the radiation then the absorbing area of that fibre is 2RL since the fibre will appear as a rectangle of length L and width 2R. However, not every fibre will be

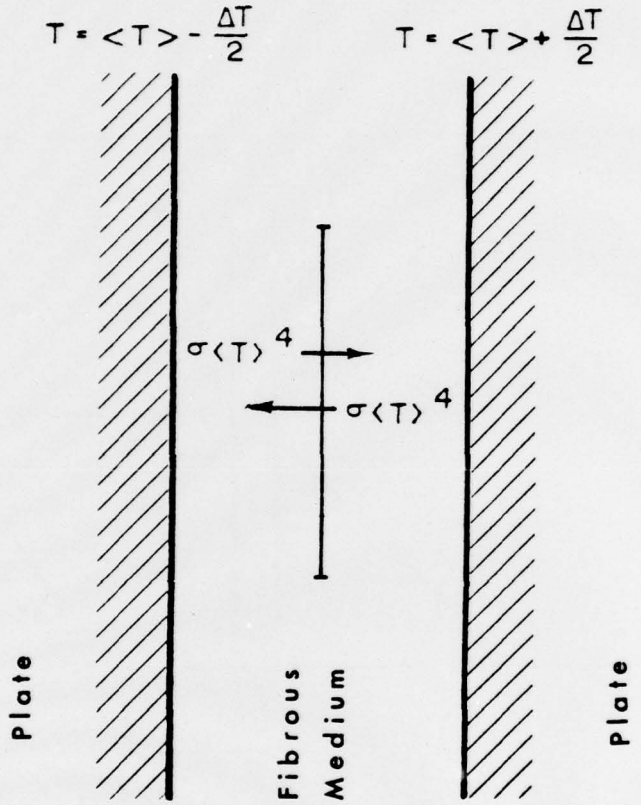

Figure 2. In an experiment the sample is between two blackened plates at known different temperatures. There is a radiative heat flux in each direction across the sample of the order of $\sigma \langle T \rangle^4$ *where* $\langle T \rangle$ *is the average temperature of the apparatus. The net radiative heat flux is much smaller than this.*

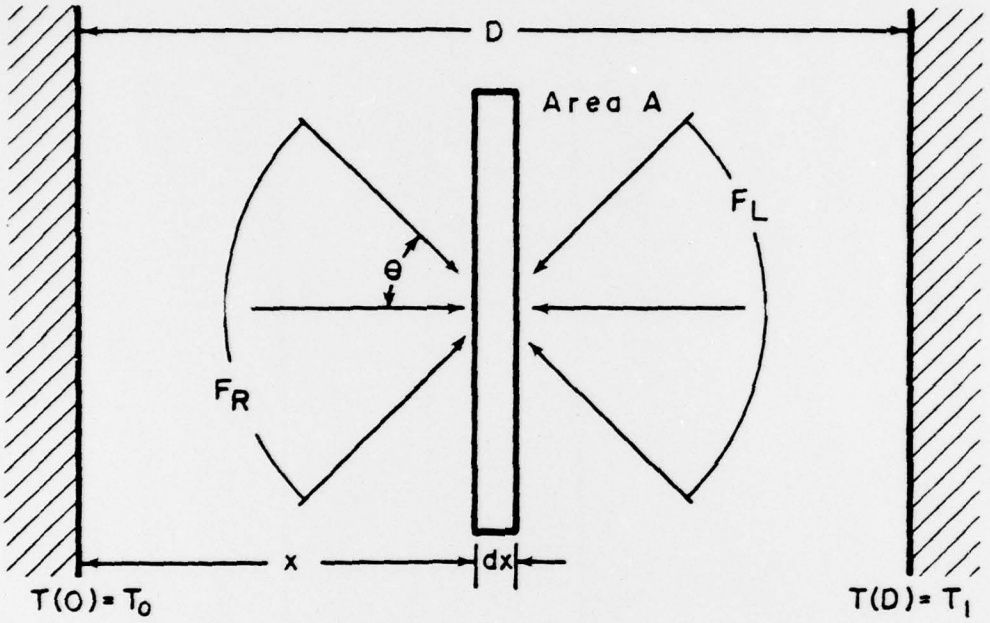

Figure 3. A volume element inside the sample is irradiated approximately isotropically. The radiant flux is, however, slightly larger from the hotter side.

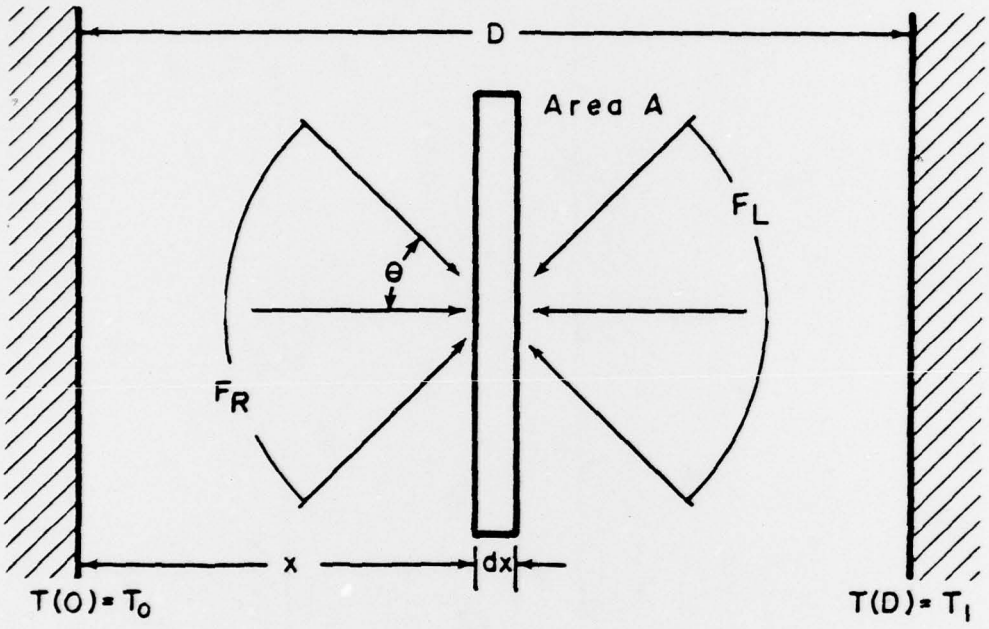

Figure 3. A volume element inside the sample is irradiated approximately isotropically. The radiant flux is, however, slightly larger from the hotter side.

so aligned; the apparent area has to be averaged over all possible orientations. This averaging introduces a factor of $\frac{\pi}{4}$ so that the average absorbing area presented by the fibres is

$$2RL \times \frac{\pi}{4} = \frac{\pi RL}{2} .$$

Now, with n fibres per unit volume and a volume Adx, the volume element presents an absorbing surface area of

$$\frac{\pi RL}{2} n \; A \; dx = \frac{f}{2R} \; A \; dx$$

If we assume that the fibres have a thermal emissivity ε, the power absorbed in dV is this area times ε times the intensity integrated over all solid angles in the left-hand half-space. The integration simply gives a factor of 2π since the intensity and area are independent of angle. Thus

(5) Power absorbed $= (2\pi)(\varepsilon) \frac{f}{2R} \; Adx \; I(x)$

$$= \frac{f\varepsilon}{R} \; Adx \; \pi \; I(x)$$

$$= \frac{f\varepsilon}{R} \; F_R \; Adx$$

In addition to absorbing radiation, the fibres radiate at temperature T(x). The total radiating area within dV is

$$2\pi R \; L \; n \; Adx = \frac{2f}{R} \; Adx$$

Therefore, the total radiation is

(6) Power Radiated $= 2 \frac{f\varepsilon}{R} \sigma \; T^4(x) \; Adx$

and this is distributed isotropically so that half of this will be into the left hand space and half into the right.

We can now relate the radiation flux, travelling to the right, that leaves the volume element at x + dx to that entering at x. The difference is the power absorbed from the left-hand half-space minus the power radiated into the right hand half-space. Thus

$$A \; F_R(x) - A \; F_R(x+dx) = \frac{f\varepsilon F_R}{R} \; Adx - \frac{f\varepsilon\sigma T^4(x)}{R} \; Adx$$

Hence

$$\frac{F_R(x+dx)-F_R(x)}{dx} = -\frac{f\epsilon}{R}F_R + \frac{f\epsilon}{R}\sigma T^4(x)$$

or (7) $$\frac{dF_R}{dx} = -\frac{f\epsilon}{R}\{F_R - \sigma T^4\}$$

A similar analysis of radiation travelling to the left gives

(8) $$\frac{dF_L}{dx} = \frac{f\epsilon}{R}\{F_L - \sigma T^4\}$$

TOTAL HEAT FLOW

Basic Equations

Heat may flow at any point either by conduction or by radiation but, since the fibres are both absorbing and radiating, heat is converted from one form to the other and the two processes, conduction and radiation, are not independent. Consider a volume element as in Figure 4. The net amount of conductive heat flowing into this element is

$$Q(x) - Q(x+dx) = -Ak\frac{dT}{dx}(x) + Ak\frac{dT}{dx}(x+dx)$$

This plus the net amount of heat being liberated in dV must be zero at steady state. This latter is the difference between the power absorbed and the power radiated

$$\frac{f\epsilon}{R}(F_R+F_L)\,Adx - \frac{2f\epsilon}{R}\sigma T^4 Adx$$

Thus

$$Ak\left[\frac{dT}{dx}(x+dx) - \frac{dT}{dx}(x)\right] + \frac{f\epsilon}{R}\{F_R+F_L - 2\sigma T^4(x)\}\,Adx = 0$$

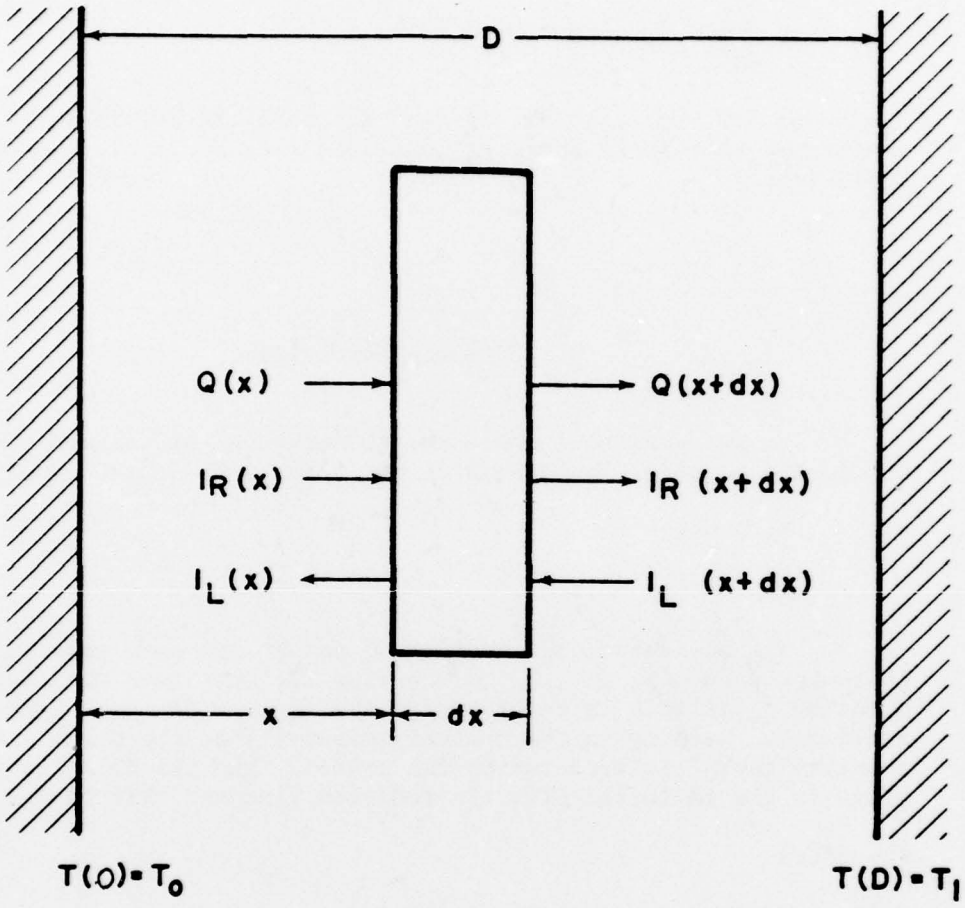

Figure 4. The flow of heat by conduction and radiation into and out of a volume element. Heat can be converted from one form to another by absorption or emission of thermal radiation.

or

$$(9) \qquad k \frac{d^2T}{dx^2} = \frac{-f\varepsilon}{R} \{F_R + F_L - 2\sigma T^4\}$$

Equations (7), (8) and (9) together describe the combined radiant and conductive heat flows and must be solved with appropriate boundary conditions.

Boundary Conditions

In an experiment where the temperatures of the two plates are known, the boundary conditions on T(x) can be specified simply:

$$(10) \qquad T(0) = T_0$$

$$T(D) = T_1$$

The boundary conditions on F_R and F_L are more complex. At the left hand boundary, x=0, F_L is the flux incident onto the plate. A fraction ε_0 of this is absorbed and the rest, a fraction $1-\varepsilon_0$, is reflected. Here ε_0 is the thermal emissivity of the plate. Also a quantity $\varepsilon_0\sigma T_0^4$ is radiated by the plate. Thus the flux leaving the plate is the reflected plus the radiated flux and this is F_R.

Therefore

$$(12) \qquad F_R(0) = (1-\varepsilon_0)F_L(0) + \varepsilon_0\sigma T_0^4$$

Similarly at the right hand plate, x=D,

$$(13) \qquad F_L(D) = (1-\varepsilon_1)F_R(D) + \varepsilon_1\sigma T_1^4$$

where ε_1 in the thermal emissivity of this plate.

Solution of Linearized Equations

A complete calculation of the combined conductive and radiative heat flow requires the solution of the equation set (7) to (13). This is a difficult task since equations (7) to (9) are non-linear, involving terms in T^4. A great simplification is brought about by approximating this T^4 term by one linear in T. Thus set:

(14) $T = t_o + t$

Then

(15) $T^4 = (t_o + t)^4 = t_o^4(1+\frac{t}{t_o})^4 \cong t_o^4(1+\frac{4t}{t_o}) = t_o^4+4t_o^3t$

If we take $t_o = \frac{T_o+T_1}{2} \cong 300$ K

then $|t| << |\frac{T_1-T_o}{2}| \cong 5$ K

and the approximation is valid to better than

$$6\left(\frac{t}{t_o}\right)^2 \quad \text{or about } 0.5\%.$$

It is also convenient to change variables to the net and total radiant heat fluxes.

(16) $F_N = F_R - F_L$

(17) $F_T = F_R + F_L$

The linearized equations then become

(18) $$\frac{dF_T}{dx} = \frac{-f\epsilon}{R} F_N$$

(19) $$\frac{dF_N}{dx} = \frac{-f\epsilon}{R} \{F_T - 2\sigma t_o^4 - 8\sigma t_o^3 t\}$$

$$(20) \qquad k \frac{d^2t}{dx^2} = \frac{dF_N}{dx}$$

The boundary conditions (10) and (11) become

$$(21) \qquad t(0) = T_o - t_o$$

$$(22) \qquad t(D) = T_1 - t_o$$

and (12) and (13) become

$$(23) \qquad \epsilon_o F_T(0) + (2-\epsilon_o) F_N(0) = 2\epsilon_o \sigma T_o^4 \cong 2\epsilon_o \sigma t_o^4 + 8\epsilon_o \sigma t_o^3 (T_o - t_o)$$

$$(24) \qquad \epsilon_o F_T(D) - (2-\epsilon_1) F_N(D) = 2\epsilon_1 \sigma T_1^4 \cong 2\epsilon_1 \sigma t_o^4 + 8\epsilon_1 \sigma t_o^3 (T_1 - t_o)$$

Equations (18) to (24) are exactly solvable.

The general solution of (18), (19) and (20) is

$$(25) \qquad t = \alpha_o + \alpha_1 x + \alpha_2 e^{-px} + \alpha_3 e^{p(x-D)}$$

$$(26) \qquad F_T = 2\sigma t_o^4 + 8\sigma t_o^3 \alpha_o + 8\sigma t_o^3 \alpha_1 x - \frac{f\epsilon k}{R} \alpha_2 e^{-px} - \frac{f\epsilon k}{R} \alpha^3 e^{p(x-D)}$$

$$(27) \qquad F_N = \frac{-R}{f\epsilon} 8\sigma t_o^3 \alpha_1 - kp\alpha_2 e^{-px} + kp\, e^{p(x-D)}$$

where $p = \frac{f\epsilon}{R} \{1 + \frac{8\sigma t_o^3}{k} \frac{R}{f\epsilon}\}^{\frac{1}{2}}$

and the constants α_1 are to be determined by the boundary conditions. Using (25) for t(x), equations (21) and (22) give

$$(28) \qquad \alpha_o + \alpha_2 + \alpha_3 e^{-pD} = T_o - t_o$$

$$(29) \qquad \alpha_o + \alpha_1 D + \alpha_2 e^{-pD} + \alpha_3 = T_1 - t_o$$

and using (26) and (27) in (23) and (24)

$$(30)\qquad 8\varepsilon_o\sigma t_o^3\alpha_0 - (2-\varepsilon_o)\frac{R}{f\varepsilon}8\sigma t_o^3\alpha_1 - k\{(2-\varepsilon_o)p + \varepsilon_o\frac{f\varepsilon}{R}\}\alpha_2$$

$$+ k\{(2-\varepsilon_o)p - \frac{f\varepsilon}{R}\}e^{-pD}\alpha_3 = 8\varepsilon_o\sigma t_o^3(T_o-t_o)$$

$$(31)\qquad 8\varepsilon_1\sigma t_o^3\alpha_0 + 8\sigma t_o^3\{(2-\varepsilon_1)\frac{R}{f\varepsilon} + \varepsilon_1 D\}\alpha_1 + k\{(2-\varepsilon_1)p - \varepsilon_1\frac{f\varepsilon}{R}\}e^{-pD}\alpha_2$$

$$- k\{(2-\varepsilon_1)p + \varepsilon_1\frac{f\varepsilon}{R}\}\alpha_3 = 8\varepsilon_1\sigma t_o(T_1-t_o)$$

Equations (28) to (31) uniquely determine α_0, α_1, α_2 and α_3 and are solved numerically for each set of parameters ε, ε_0, ε_1, T_o, T_1, f and R. The value of t_o is chosen to be $(T_o + T_1)/2$.

EXPERIMENT

Thermal resistance measurements were made on an apparatus almost identical to that described by Clulow and Rees (1). The technique consists basically of measuring the temperature drops across the sample and a standard of known thermal resistance when these are held in contact with each other in series between two blackened plates at known, different temperatures. The limit to the accuracy of this apparatus is the error ($\pm$ .05°C) in the temperature measurements which are made with copper-constantan thermcouples.

The first set of experiments was performed without a sample in place in order to measure the thermal resistance of air gaps of various thicknesses in order to determine the thermal emissivity of the blackened surfaces, a number required as input to the numerical calculations. A similar set of measurements was made with one blackened surface covered by a sheet of aluminum foil. This was done to determine the emissivity of the foil so that the prediction of effect of surface emissivity on the resistance of a sample could be checked.

TABLE I

Material Parameters Used in the Model Calculations

Batting	Fibre Content	Mass (g/m^2)	Average Fibre Radius (μm)	Fibre Specific Gravity	Fibre Thermal Conductivity W/m K	Nominal Thickness[4] (mm)	% Fibre at Nominal Thickness
Polarguard [1]	Polyester	270	11.7	1.38	0.159	26	0.75
Holofil [2]	Polyester	350	13.2	1.38	0.159	28	0.91
Thinsulate [3]	Polypropylene	545	1.5	0.91	0.117	7.7	5.8

1. Supplied by Celanese Canada Ltd.
2. Supplied by DuPont of Canada Ltd.
3. Supplied by 3M Canada Ltd.
4. Measured at 0.16 kPa (CAN2-4.2-M77, Method 37)

Next, the resistance of one sample of each of the 3 battings was measured at various values of compression and, in the case of Polarguard, with and without the foil in place. Finally, resistance measurements were made, at fixed compression, of several samples of different weights of each of the battings. The pertinent physical properties of the three battings are given in Table I.

RESULTS AND DISCUSSION

Air Gaps

The resistances of air gaps in the thickness range 1 to 13 mm are shown in Figure 5. For an air gap in which there is no convection one expects a heat flow Q_T per unit area given by

$$(32) \qquad Q_T = k_A \frac{(T_1 - T_o)}{D} + \frac{\sigma \varepsilon_o \varepsilon_1}{\varepsilon_o + \varepsilon_1 - \varepsilon_o \varepsilon_1} (T_1^4 - T_o^4)$$

where k_A is the thermal conductivity of air

D is the air gap thickness

σ is the Stefan-Boltzmann Constant

and ε_o, ε_1, T_o and T_1 are the emissivities and temperatures, respectively, of the two plates.

In Figure 5 the theoretical line has been calculated according to equation (32) with a value of $\varepsilon_o = \varepsilon_1 = 0.92$ which has been selected to give best agreement between theory and experiment in the region from 2 to 12 mm. Within this region the agreement is within experimental error but the two end points, at thicknesses of 1 and 13 mm, deviate significantly. At the 1-mm point this deviation is almost certainly instrumental in origin since it is difficult to conceive of any mechanism that would give a resistance greater than that predicted by equation (32). Indeed there was some slight error in the apparatus that gave a finite resistance reading even at zero gap thickness. At the other end of the curve, the deviation is in the other direction; the measured value is markedly lower than predicted. This can be explained as the onset of convective heat transfer at large gap thickness.

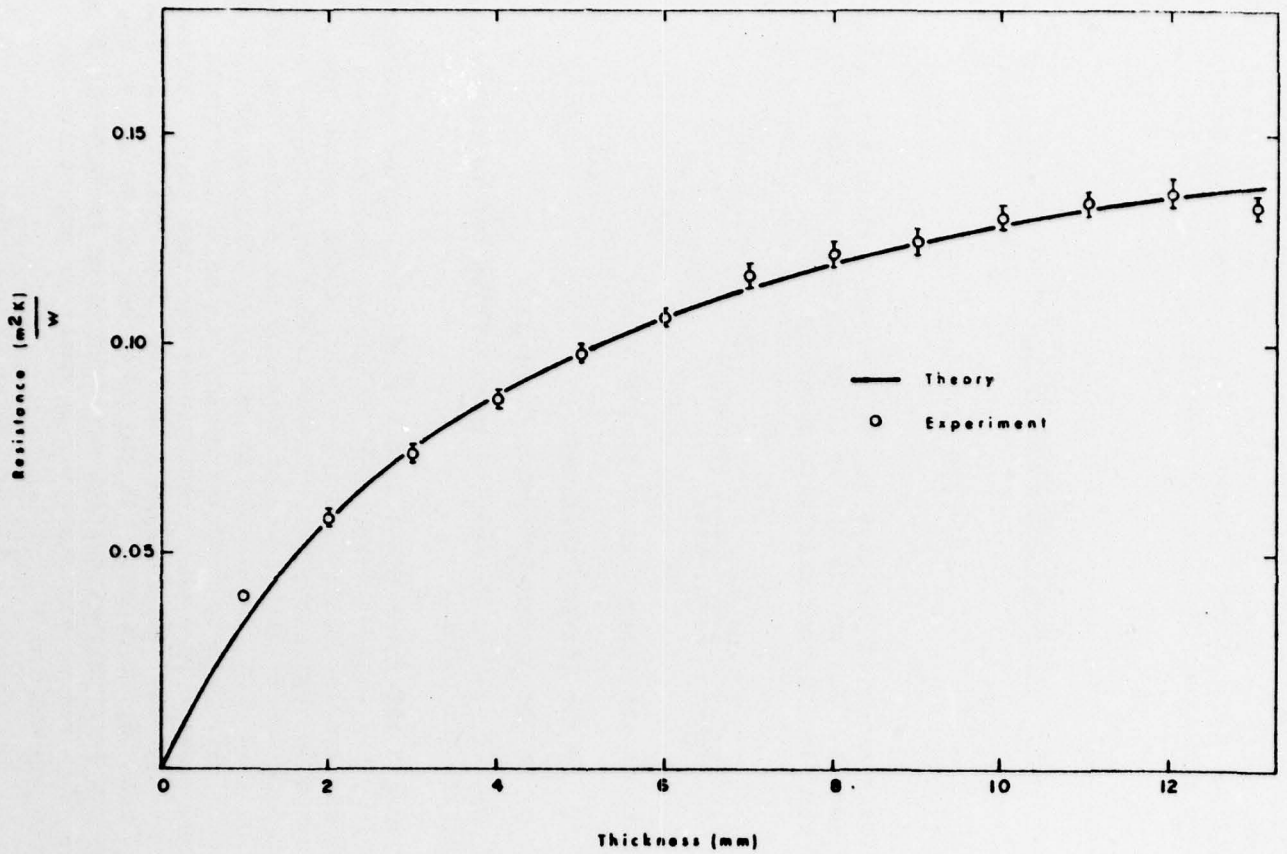

Figure 5. The thermal resistance of horizontal air gaps between two blackened surfaces. The theory is based on the assumptions of conductive and radiative heat transfer only and a value for the thermal emissivity of each of the surfaces of 0.92. The experimental error is dominated by the accuracy of the temperature measurements.

It is concluded from the data of Figure 5 that convection was negligible in this apparatus for spacing without a sample of up to 12 mm thickness and that the two blackened surfaces had emissivities (assumed to be equal) of 0.92. The error in this figure is about ± 0.01.

Measurements with a sheet of foil in place gave results very similar to Figure 5 with a value of ε for the foil of 0.05 ± 0.01.

POLARGUARD

Resistance data for a sample of Polarguard whose compression, and thus thickness, was varied are shown in Figure 6. Here the sample was between two blackened surfaces with separations in the range from 4 to 26 mm. Unfortunately the theory cannot be used to unambiguously predict the thermal resistance since the value of ε, the thermal emissivity of a single fibre, is not available. Therefore $\varepsilon=0.56$ was chosen to give agreement between experiment and theory at the greatest plate separation (26 mm). As can be seen from Figure 6, the theory then predicts the resistance at all other points within experimental error.

A similar set of data for the same sample but with a sheet of aluminum foil in place is shown in Figure 7. Here the calculations have been made using the same value of ε, the emissivity of the fibres, as was determined previously for the two black surface case. This experiment was performed since it brings about a change in the radiative contribution to the heat flow at the surface of the plate while leaving the conductive contribution the same thus subjecting the theory to a severe test. Unfortunately the test was not as severe as might be wished since the change in resistance brought about by replacing a blackened surface with a reflecting one was only about 5%, about the same size as the experimental error. Nevertheless, the approximate size of change is predicted correctly by the theory.

It should be noted that the splitting of the heat transfer into conductive and radiative contributions when discussing the resistance of the sample as a whole is fictional. The conductive and radiative contributions vary from point to point within the sample, although their total, of course, remains constant.

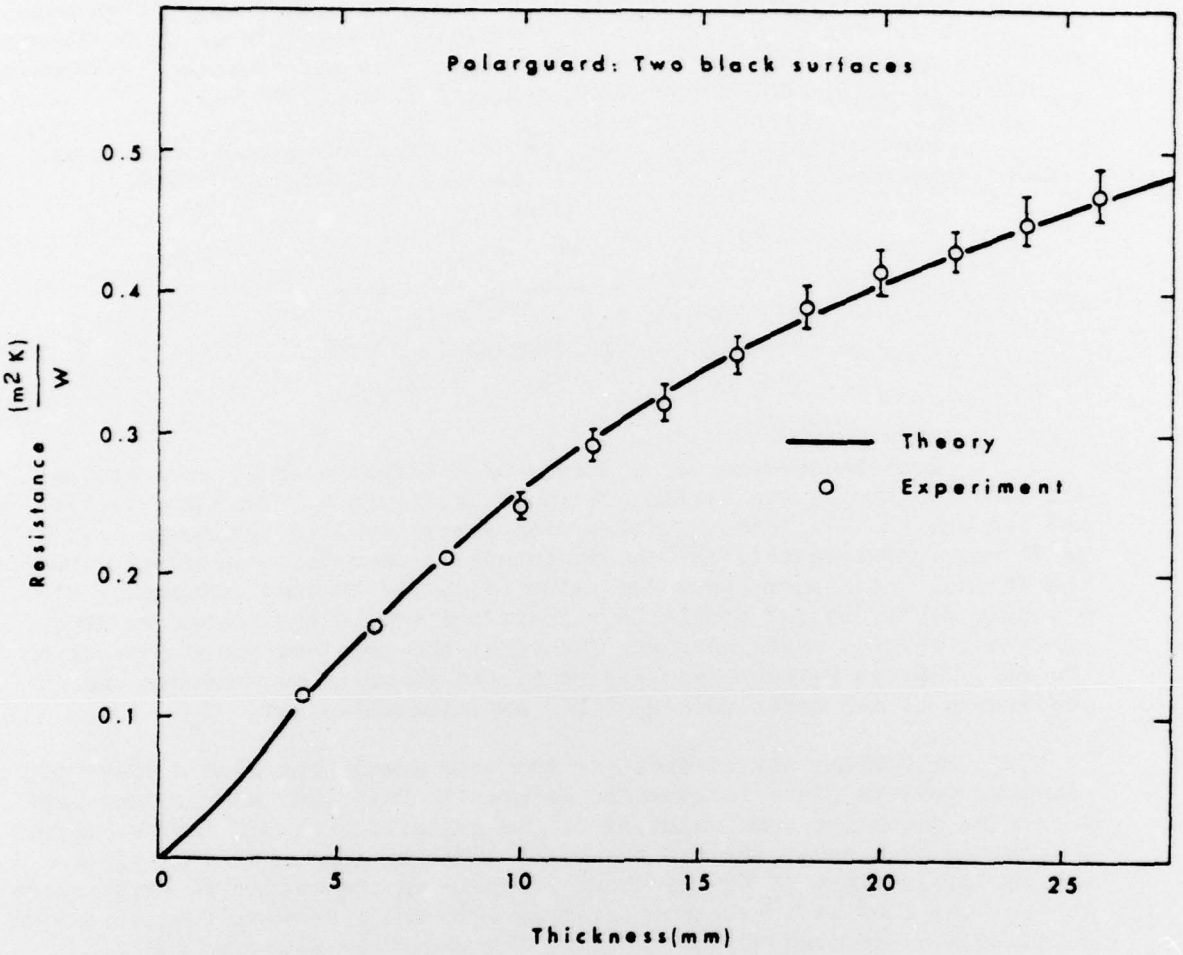

Figure 6. The variation with compression of the resistance of a sample of Polarguard between 2 blackened surfaces. The theory uses a value of fibre emissivity, ε=0.56, picked to fit the point at 26 mm thickness.

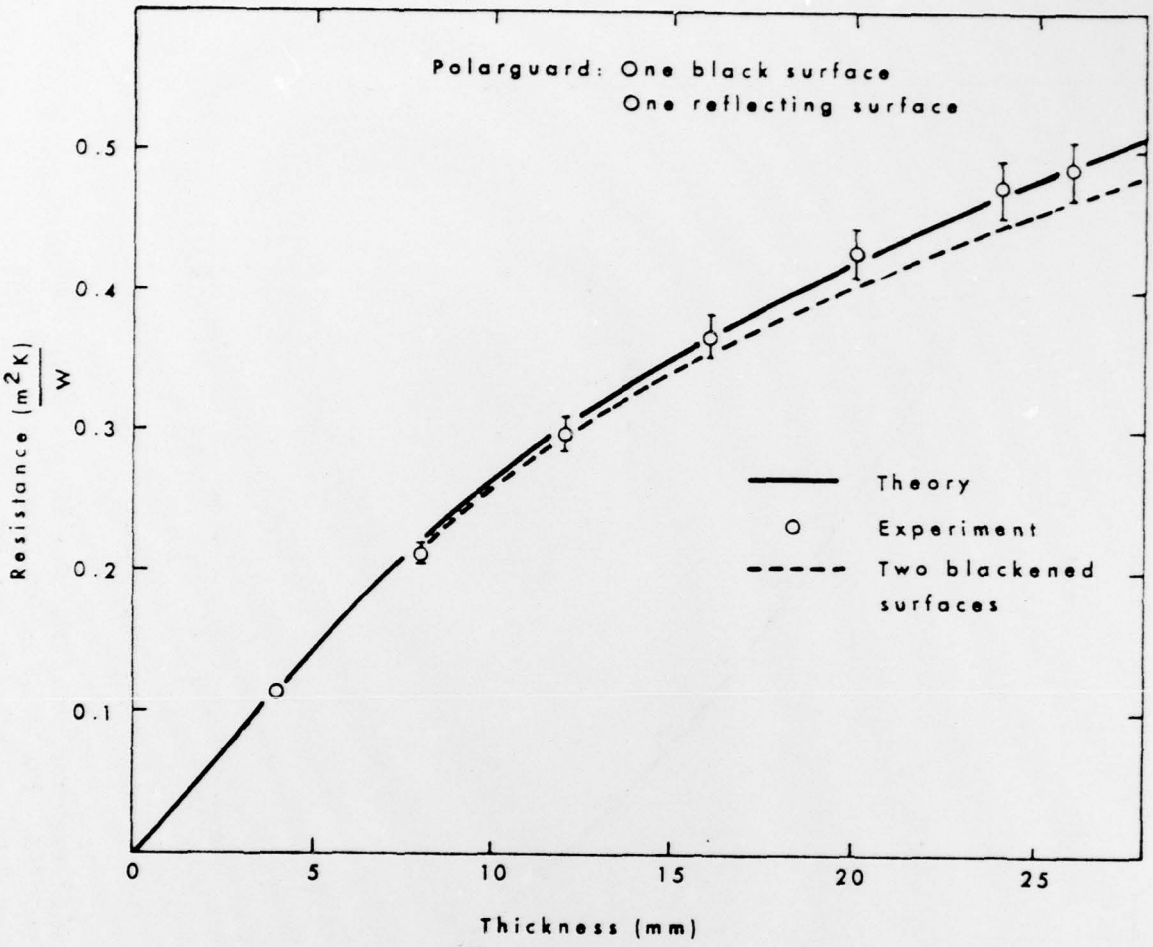

Figure 7. The variation with compression of the resistance of a sample of Polarguard between one blackened and one reflecting surface. The calculation uses only parameters whose values have been determined previously. The effect of the reflecting surface was to raise the resistance of the sample by 5% at large thicknesses over the values for two blackened surfaces.

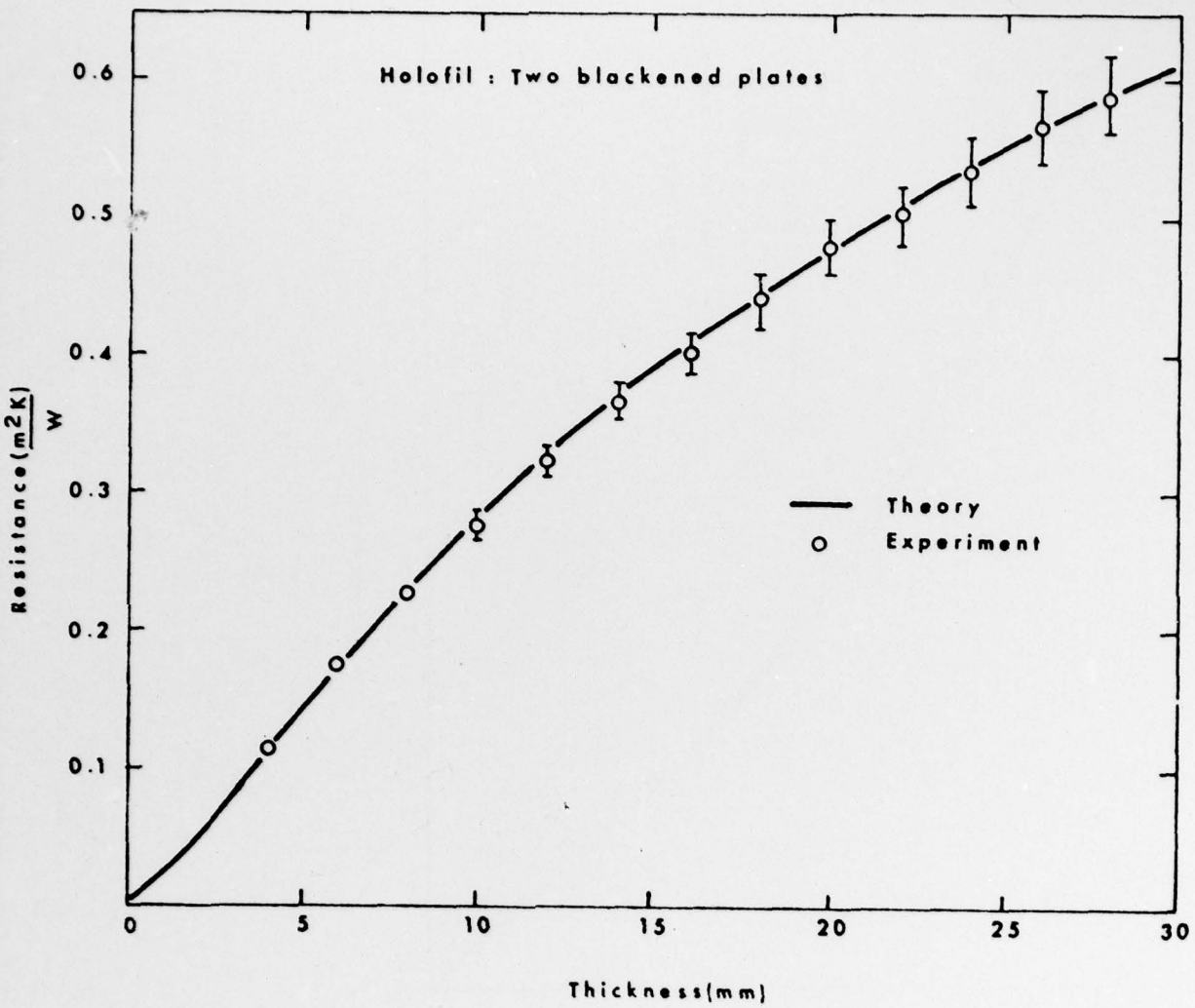

Figure 8. Variation with compression of the thermal resistance of a sample of Holofil. The calculation uses a value of fibre emissivity of 0.65, adjusted to fit the point at 28 mm.

In this sample of Polarguard at thicknesses of about 20 mm, the theory shows that the radiative and conductive contributions to the heat transfer are of comparable size. Therefore the small size of the resistance change with a change from a black to a reflecting surface is, of itself, worthy of note and is discussed in more detail below.

The uncertainty in the value of ε derived from these data is ± 0.03.

HOLOFIL

The data for a sample of Holofil under varying degrees of compression are shown in Figure 8. Again the theory has been adjusted to fit the experimental point at the greatest plate separation (28 mm). As before the theory agrees with the other points within error. The value of ε used here is 0.69 and the uncertainty in this figure is about ± 0.03.

The calculation for Holofil is slightly complicated by its hollow core (about 10% of the volume of the fibre). This space has been treated as part of the fraction of the batting that is air for the purposes of calculating conductive heat flow and ignored in the calculation of radiative heat flow. Thus the effective fractional fibre volume used in the calculation of radiation is slightly larger than that used in the calculation of conduction. This is done for convenience and undoubtedly introduces a slight error into the calculations.

THINSULATE

The results of an experiment on a sample of Thinsulate are shown in Figure 9. The high incompressibility of this material prevented a wide range of thicknesses being obtained so the results are somewhat inconclusive. Again the value of ε has been chosen to fit the point at maximum thickness (7.7 mm). Here, significant deviations of the observed resistances from the prediction are evident at low values of thickness. This is probably due to the breakdown of the theory due to inadequate treatment of fibre conduction at large fractional fibre volumes (45% at 4.2 mm).

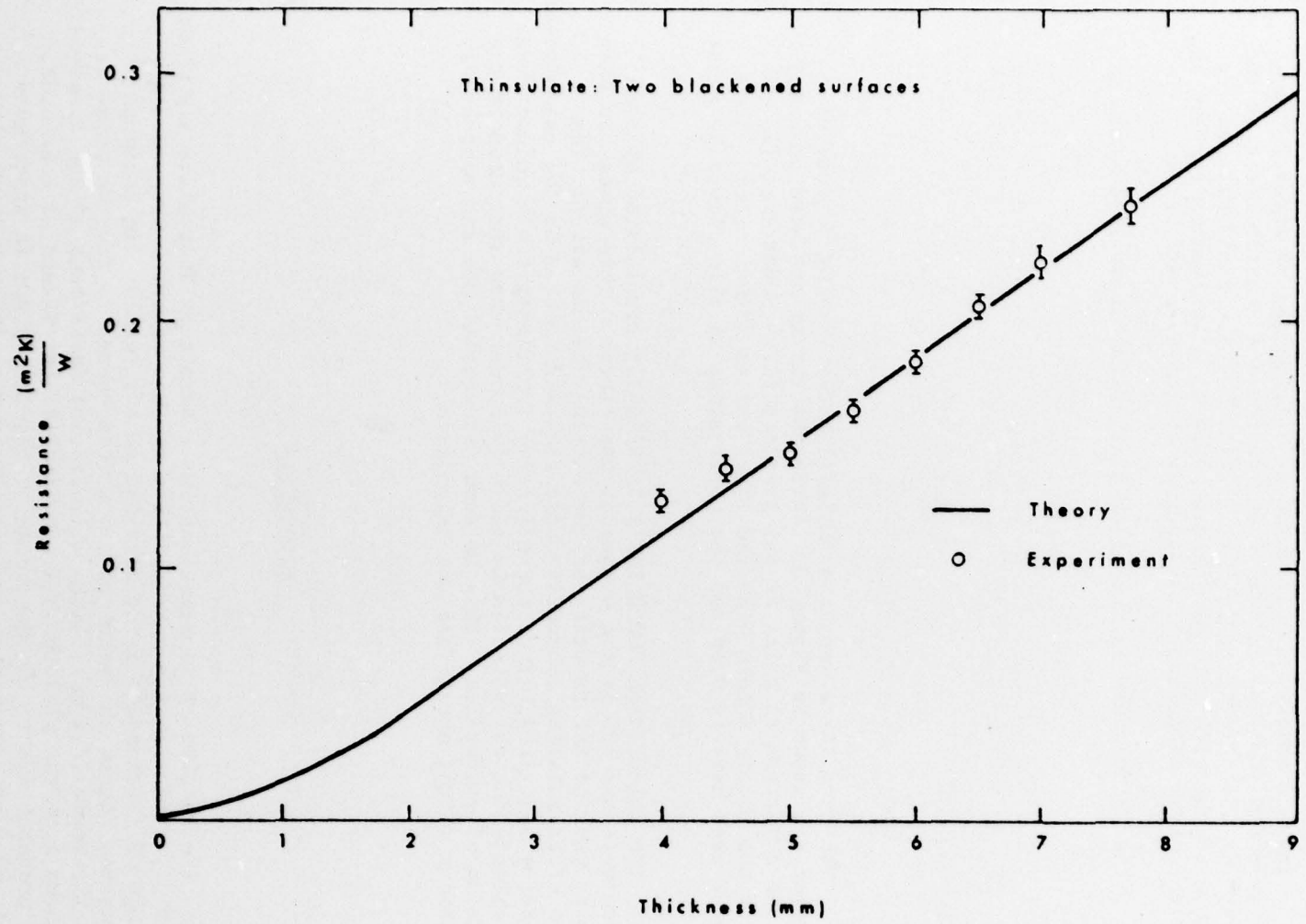

Figure 9. The variation with compression of the resistance of a sample of Thinsulate. The theory uses a value of fibre emissivity ε=0.18, adjusted to fit the point at 7.7 mm. Some deviation of the experiment from the calculation is observed at low values of thickness. This is possibly due to a breakdown of the theory for large fractional fibre content.

The value of ε used here is 0.18 but this is a highly uncertain figure. Since, as is discussed below, Thinsulate is highly opaque to thermal radiation, the predictions of the theory are insensitive to the parameter ε so that its determination from the data is inaccurate. The value quoted here is therefore only certain within a factor of 2 or so. Nevertheless, ε for Thinsulate is significantly less than for Polarguard or Holofil, undoubtedly due to the smaller fibre diameter (3 vs 20μm).

ADDITIONAL SAMPLES

Results at a fixed thickness for several other samples of each of the three battings are summarized in Table II. The calculations use the values of ε derived from the previous experiments. In about half the cases the theory and experiment agree within error but in the others the prediction is out by a few percent, consistently on the low side. Also in the cases where agreement was within error the prediction is lower than the mean experimental result. This indicates some systematic error either in the experiment or the theory. Since the error is so small and no explanation is immediately apparent, it does not seem worthwhile embarking on a long search for its cause.

The general agreement between the experimental and calculated values of thermal resistance for these battings supports the theory that is presented. In particular the exclusion of convection from the theory is vindicated. This is not surprising once it is observed that convection is negligible for air gaps up to 12 mm thickness. One would not expect the insertion of fibres into the space to introduce convection, hence convection would not be expected for batting thickness at least up to 12 mm and possibly up to the 28 mm thickness used here. Of course it is still possible that convection might be important in samples thicker than those used in this study.

Since the theory agrees well with the results for all three battings it can be used to understand the difference in thermal resistance between Thinsulate and the conventional battings. The difference, according to the model, lies primarily in the different opacity of the materials to thermal radiation but since the two mechanisms, conduction and radiation, are closely interrelated it is not possible to make a comparison of materials by quoting separate values of conductive and radiative heat transfer for each sample. Some insight can be gained, however, by considering the ideal case of a very thick sample.

TABLE II

Material Properties and Experimental and Calculated Resistances for Several Samples of the Three Battings

Sample		Mass (g/m^2)	Thickness (mm)	Fibre Content (%)	Experimental Resistance (m^2 K/W)	Calculated Resistance (m^2 K/W)	$\frac{\text{Expt.Res}}{\text{Thickness}}$ (m K/W)	$\beta = \frac{f\epsilon}{\bar{R}}$ (m^{-1})
Polarguard	#1	220	20.2	0.78	0.399 ±0.023	0.377	19.8	374
	#2	295	25.0	0.86	0.485 ±0.013	0.478	19.4	412
	#3	115	12.4	0.90	0.272 ±0.014	0.257	21.9	432
	#4	255	24.2	0.76	0.462 ±0.013	0.439	19.1	365
	#5	270	26.3	0.74	0.478 ±0.013	0.469	18.2	355
Holofil	#1	185	12.2	1.10	0.283 ±0.010	0.287	23.5	636
	#2	260	22.0	0.86	0.493 ±0.020	0.458	20.8	497
	#3	350	27.4	0.93	0.602 ±0.018	0.582	21.2	537
Thinsulate	M530	545	8.5	7.1	0.268 ±0.005	0.266	31.5	8520
	M400	405	7.7	5.8	0.249 ±0.005	0.248	32.3	6960
	M200	200	3.5	6.3	0.122 ±0.002	0.111	34.8	7560

Far from the boundaries at x=0 and x=D we have in equations (25) to (27)

$$px >> 1$$

and $$-p(x-D) >> 1$$

where p is as defined previously, so that the exponential terms are small

$$e^{-px} \cong 0$$

$$e^{p(x-D)} \cong 0$$

Then the solutions for t and F_N are

(33) $$t = \alpha_0 + \alpha_1 x$$

(34) $$F_N = \frac{-R 8\sigma\alpha_1}{f\epsilon}$$

Equation (33) just represents a linearly varying temperature with gradient

$$\frac{dT}{dx} = \alpha_1$$

So that (34) becomes

(35) $$F_N = \frac{-R}{f\epsilon} 8\sigma t_o^3 \frac{dT}{dx}$$

F_N is then proportional to temperature gradient and depends on the quantity β where

(36) $$\frac{1}{\beta} = \frac{R}{f\epsilon}$$

The parameter β is then a measure of the opacity of the material; the greater is β the more opaque is the material and the less important is the radiation to the overall thermal transport.

In Table II the values of β are quoted for each material and these can be compared to the resistance per unit thickness. Indeed, both the resistance per unit thickness and β are very much larger for Thinsulate than for the other two battings.

The quantity β can be interpreted as an effective absorption constant for the medium. If an intensity of radiation I_o is incident on the surface, the intensity will decay exponentially with distance inside the batting as

$$I = I_o e^{-\beta x} \tag{36}$$

The values of β for Polarguard are in the range 300 to 400 m^{-1} so that the radiation at the surface is all absorbed in about the first $\frac{1}{300}$ m or 3mm. This explains why the changing of emissivity of one of the surfaces from black to highly reflecting produced only a 5% change in the resistance of Polarguard. The radiant flux changed in only the first few millimetres of a sample which was up to 26 mm thick.

Radiation is an important heat transfer mechanism not because radiation passes through the sample but because heat is transferred within the sample from fibre to fibre by radiation as well as by conduction.

CONCLUSION

The theory presented in this paper successfully explains the observed values of the thermal resistance of the three battings in terms of a combined flow of heat by conduction and radiation and without the inclusion of convection being required. The relatively high value of the thermal resistance per unit thickness of Thinsulate is explained by its high opacity to thermal radiation.

REFERENCES

1. E.E. Clulow and W.H. Rees, J. Text. Inst. 59, 285 (1968).

UNCLASSIFIED

Security Classification

DOCUMENT CONTROL DATA - R & D

(Security classification of title, body of abstract and indexing annotation must be entered when the overall document is classified)

1. ORIGINATING ACTIVITY
Defence Research Establishment Ottawa
National Defence Headquarters
Ottawa, Ontario Canada K1A 0Z4

2a. DOCUMENT SECURITY CLASSIFICATION
Unclassified

2b. GROUP

3. DOCUMENT TITLE
Measurements and Calculations of the Thermal Resistance of Three Synthetic-Fibre Battings (U)

4. DESCRIPTIVE NOTES (Type of report and inclusive dates)
Report

5. AUTHOR(S) (Last name, first name, middle initial)
Farnworth, B., Crow, R.M., Dewar, M.M.

6. DOCUMENT DATE
November 1979

7a. TOTAL NO. OF PAGES
25

7b. NO. OF REFS
1

8a. PROJECT OR GRANT NO.
14B30

9a. ORIGINATOR'S DOCUMENT NUMBER(S)
DREO Report No. 818

8b. CONTRACT NO.

9b. OTHER DOCUMENT NO.(S) (Any other numbers that may be assigned this document)

10. DISTRIBUTION STATEMENT
Unlimited

11. SUPPLEMENTARY NOTES

12. SPONSORING ACTIVITY

13. ABSTRACT (U)

A theory of the combined transport of heat by radiation and by conduction in fibrous media is presented. The theory agrees well with the differences between them without the inclusion of convective heat transfer being required.

DSIS
72-508

Security Classification

KEY WORDS

INSTRUCTIONS

1. ORIGINATING ACTIVITY: Enter the name and address of the organization issuing the document.

2a. DOCUMENT SECURITY CLASSIFICATION: Enter the overall security classification of the document including special warning terms whenever applicable.

2b. GROUP: Enter security reclassification group number. The three groups are defined in Appendix 'M' of the DRB Security Regulations.

3. DOCUMENT TITLE: Enter the complete document title in all capital letters. Titles in all cases should be unclassified. If a sufficiently descriptive title cannot be selected without classification, show title classification with the usual one-capital-letter abbreviation in parentheses immediately following the title.

4. DESCRIPTIVE NOTES: Enter the category of document, e.g. technical report, technical note or technical letter. If appropriate, enter the type of document, e.g. interim, progress, summary, annual or final. Give the inclusive dates when a specific reporting period is covered.

5. AUTHOR(S): Enter the name(s) of author(s) as shown on or in the document. Enter last name, first name, middle initial. If military, show rank. The name of the principal author is an absolute minimum requirement.

6. DOCUMENT DATE: Enter the date (month, year) of Establishment approval for publication of the document.

7a. TOTAL NUMBER OF PAGES: The total page count should follow normal pagination procedures, i.e., enter the number of pages containing information.

7b. NUMBER OF REFERENCES: Enter the total number of references cited in the document.

8a. PROJECT OR GRANT NUMBER: If appropriate, enter the applicable research and development project or grant number under which the document was written.

8b. CONTRACT NUMBER: If appropriate, enter the applicable number under which the document was written.

9a. ORIGINATOR'S DOCUMENT NUMBER(S): Enter the official document number by which the document will be identified and controlled by the originating activity. This number must be unique to this document.

9b. OTHER DOCUMENT NUMBER(S): If the document has been assigned any other document numbers (either by the originator or by the sponsor), also enter this number(s).

10. DISTRIBUTION STATEMENT: Enter any limitations on further dissemination of the document, other than those imposed by security classification, using standard statements such as:

    (1) "Qualified requesters may obtain copies of this document from their defence documentation center."

    (2) "Announcement and dissemination of this document is not authorized without prior approval from originating activity."

11. SUPPLEMENTARY NOTES: Use for additional explanatory notes.

12. SPONSORING ACTIVITY: Enter the name of the departmental project office or laboratory sponsoring the research and development. Include address.

13. ABSTRACT: Enter an abstract giving a brief and factual summary of the document, even though it may also appear elsewhere in the body of the document itself. It is highly desirable that the abstract of classified documents be unclassified. Each paragraph of the abstract shall end with an indication of the security classification of the information in the paragraph (unless the document itself is unclassified) represented as (TS), (S), (C), (R), or (U).

    The length of the abstract should be limited to 20 single-spaced standard typewritten lines; 7½ inches long.

14. KEY WORDS: Key words are technically meaningful terms or short phrases that characterize a document and could be helpful in cataloging the document. Key words should be selected so that no security classification is required. Identifiers, such as equipment model designation, trade name, military project code name, geographic location, may be used as key words but will be followed by an indication of technical context.